



Published in final edited form as:

J Refract Surg. 2009 September ; 25(9): 776–786. doi:10.3928/1081597X-20090813-04.

Stromal Thickness in the Normal Cornea: Three-dimensional Display With Artemis Very High-frequency Digital Ultrasound

Dan Z. Reinstein, MD, MA(Cantab), FRCSC, FRCOphth, Timothy J. Archer, MA(Oxon), DipCompSci(Cantab), Marine Gobbe, MST(Optom), PhD, Ronald H. Silverman, PhD, and D. Jackson Coleman, MD

London Vision Clinic (Reinstein, Archer, Gobbe) and the Department of Ophthalmology, St Thomas' Hospital - Kings College (Reinstein), London, United Kingdom; the Department of Ophthalmology, Weill Cornell Medical College, (Reinstein, Silverman, Coleman); Riverside Research Institute (Silverman), New York, NY; and Centre Hospitalier National d'Ophthalmologie, Paris, France (Reinstein)

Abstract

PURPOSE—To characterize the stromal thickness profile in a population of normal eyes.

METHODS—Stromal thickness profile was measured in vivo by Artemis very high-frequency digital ultrasound scanning (ArcScan, Morrison, Colo) across the central 10-mm corneal diameter on 110 normal eyes. Maps of the average, standard deviation, minimum, maximum, and range of stromal thickness were plotted. The average location of the thinnest stroma was found. The cross-sectional hemi-meridional stromal thickness profile was calculated using annular averaging. The absolute stromal thickness progression relative to the thinnest point was calculated using annular averaging as well as for 8 hemi-heridians individually.

RESULTS—The mean stromal thickness at the corneal vertex and at the thinnest point were $465.4 \pm 36.9 \mu\text{m}$ and $461.8 \pm 37.3 \mu\text{m}$, respectively. The thinnest stroma was displaced on average 0.17 ± 0.31 mm inferiorly and 0.33 ± 0.40 mm temporally from the corneal vertex. The average absolute stromal thickness progression from the thinnest point could be described by the quadratic equation: stromal thickness = $6.411 \times \text{radius}^2 + 2.444 \times \text{radius}$ ($R^2 = 0.999$). Absolute stromal thickness progression was independent of stromal thickness at the thinnest point. The increase in hemi-meridional absolute stromal thickness progression was greatest superiorly and lowest temporally.

CONCLUSIONS—Three-dimensional thickness mapping of the corneal stroma and stromal thickness progression in a population of normal eyes represent a normative data set, which may help in early diagnosis of corneal abnormalities such as keratoconus and pellucid marginal degeneration. Absolute stromal thickness progression was found to be independent of stromal thickness.

The human corneal stroma represents approximately 90% of the total corneal thickness and has an accepted central thickness of approximately 478 to 500 μm .¹⁻³ Knowledge of the stromal thickness profile is of interest in the area of corneal refractive surgery, as changes in corneal refractive power are achieved through changes in the stromal thickness profile. Measurements

Correspondence: Dan Z. Reinstein, MD, MA(Cantab), FRCSC, FRCOphth, London Vision Clinic, 8 Devonshire Pl, London W1G 6HP, United Kingdom. Tel: 44 207 224 1005; Fax: 44 207 224 1055; E-mail dzzr@londonvisionclinic.com.

Drs Reinstein, Silverman, and Coleman have a proprietary interest in the Artemis technology (ArcScan Inc, Morrison, Colo) through patents administered by the Cornell Research Foundation, Ithaca, NY. The remaining authors have no proprietary or financial interest in the materials presented herein.

Preparation in part fulfillment of the requirements for the doctoral thesis, University of Cambridge, for Dr Reinstein.

Some of the aspects of this study were presented at the American Academy of Ophthalmology Annual Meeting; November 11-14, 2006; Las Vegas, Nev.

of stromal thickness profile pre- and postoperatively allow stromal ablation rate to be quantified and changes in thickness profile to be determined.^{4,5} Stromal thickness mapping could help further understand corneal biomechanics. Stromal thickness profiles could also be useful in identifying corneal disorders such as keratoconus; corneal thickness profile has previously been suggested for the early diagnosis of keratoconus⁶ following characterization of corneal thickness progression by Mandell in 1969.⁷

Different methods have been used to measure stromal thickness: optical coherence tomography,^{8,9} confocal microscopy,^{1-3,10} and through focusing confocal microscopy.^{11,12} All studies measured the average central stromal thickness. Only two studies provided stromal thickness measurements in the peripheral cornea; however, the number of points measured was limited to one point in the temporal cornea.^{1,2}

Very high-frequency (VHF) digital ultrasound is, to date, the only published method measuring the stromal thickness profile in vivo continuously over a 10-mm diameter, measured from the anterior surface of Bowman's layer to the posterior surface of the endothelium. Very high-frequency digital ultrasound technology has gradually improved both in precision and in area of acquisition. The repeatability of corneal thickness measurements in 10 consecutive examinations of 1 eye using the Artemis I VHF digital ultrasound arc-scanning system (ArcScan Inc, Morrison, Colo) has been shown to be less than 8 μm within the central 8-mm diameter, with a central repeatability of 1.5 μm .¹³ The repeatability of epithelial thickness measurements has been shown to be less than 1.30 μm within the central 8-mm diameter, with a central repeatability of 0.5 μm .¹³

We have previously described the use of VHF digital ultrasound to measure stromal thickness before and after LASIK^{4,13-16} to investigate stromal changes induced by laser refractive surgery and compare the intended ablation depth to the achieved stromal change. We have also used VHF digital ultrasound to examine the stromal layer before and after implantation of intracorneal ring segments and demonstrated anatomical changes that were induced.¹⁷

We have previously described the thickness profile of the corneal epithelium in a population of normal eyes with no ocular pathology other than refractive error.¹⁸ The purpose of this study was to characterize the thickness profile of the corneal stroma in the same population.

PATIENTS AND METHODS

Patients

This retrospective, noncomparative cases series is from a population of patients seeking refractive surgery at the London Vision Clinic between January 2003 and December 2005. A complete ocular examination was performed to screen for corneal abnormalities and determine patient candidacy for refractive surgery. Patients with ocular pathologies such as keratoconus, corneal scars, corneal dystrophies, and previous ocular surgery were excluded. The preoperative assessment of all patients included manifest refraction, logMAR best spectacle-corrected visual acuity (BSCVA) (CSV-1000 Vector Vision Inc, Greenville, Ohio) and cycloplegic refraction using one drop of tropicamide 1% (Alcon Laboratories Ltd, Hemel Hempstead, United Kingdom). Topography and keratometry were assessed using the Orbscan II (Bausch & Lomb, Salt Lake City, Utah). Dynamic pupillometry was carried out using the Procyon P2000 pupillometer (Procyon Instruments, London, United Kingdom). Wavefront assessment was performed using the WASCA aberrometer (Carl Zeiss Meditec AG, Jena, Germany). Single-point pachymetry was measured with the Corneo-Gage Plus (50 MHz) handheld ultrasound pachymeter (Sonogage, Cleveland, Ohio) by determining the minimum of 10 consecutive central corneal measurements. Three-dimensional stromal thickness for the central 8- to 10-mm diameter was measured using the Artemis 1 technology.

Patients who met at least one of the following inclusion criteria were enrolled in the study: patients whose corneal thickness might not be sufficient to perform LASIK based on manual pachymetry measurements (ie, the residual stromal thickness predicted was less than 260 μm); high myopic patients; patients with a higher chance of requiring retreatment regardless of corneal thickness (high myopia or high cylinder); and by recruiting normal volunteers from our clinical refractive surgery practice to broaden the distribution of refraction.

Informed consent was obtained from the patient. The study was performed in accordance with an Institutional Review Board approved protocol.

Artemis VHF Digital Ultrasound Arc-scanning

The Artemis VHF digital ultrasound system has been described previously in detail in our article measuring epithelial pachymetric topography of the normal cornea.¹⁸ Briefly, Artemis VHF digital ultrasound is carried out using an ultrasonic standoff medium. The patient sits and positions the chin and forehead into a headrest while placing the eye in a soft rimmed eyecup. Warm sterile normal saline (33°C) is filled into the darkened scanning chamber. The patient fixates on a narrowly focused aiming beam, which is coaxial with the infra-red camera, corneal vertex, and center of rotation of the scanning system. The technician adjusts the center of rotation of the system until it is coaxial with the corneal vertex. In this manner, the position of each scan plane is maintained about a single point on the cornea and corneal mapping is therefore centered on the corneal vertex. The Artemis VHF digital ultrasound uses a broadband 50 MHz VHF ultrasound transducer (bandwidth approximately 10 to 60 MHz), which is swept by a reverse arc high-precision mechanism to acquire B-scans as arcs that follow the surface contour of anterior or posterior segment structures of interest. Performing a three-dimensional scan set with the Artemis 1 takes approximately 2 to 3 minutes per each eye.

Using VHF digital ultrasound, interfaces between tissues are detected at the location of the maximum change in acoustic impedance (the product of the density and the speed of sound). It was first demonstrated in 1993 that acoustic interfaces being detected in the cornea were located spatially at the epithelial surface and at the interface between epithelial cells and the anterior surface of Bowman's layer.¹⁹ This indicated that stromal thickness measurement with VHF digital ultrasound includes Bowman's layer. The posterior boundary of the stroma with VHF digital ultrasound is located at the interface between the endothelium and the aqueous, as this is the location of the maximum change in acoustic impedance. This indicated that stromal thickness measurement with VHF digital ultrasound includes Descemet's and the endothelium.

Three-dimensional Stromal Pachymetric Topography

For three-dimensional scan sets, the scan sequence consisted of four meridional B-scans at 45° intervals. Each scan sweep takes approximately 0.25 seconds and consists of 128 scan lines or pulse echo vectors. Ultrasound data are digitized and stored. The digitized ultrasound data are then transformed using patented Cornell University digital signal processing technology, which includes auto-correlation of back surface curvatures to center and align the meridional scans. A speed of sound constant of 1640 m/s was used.

Statistical Analysis

Descriptive statistics (average, minimum, maximum, standard deviation, and range) were calculated for each point in the 10×10-mm Cartesian matrix across eyes. These statistics were calculated for right eyes only, for left eyes only, and for all eyes using vertical mirrored symmetry superimposition; stromal thickness values for left eyes were reflected in the vertical axis and superimposed onto the right eye values so that nasal/temporal characteristics could be combined. The resultant matrices were plotted using DeltaGraph v5.0 (SPSS Inc, Chicago, Ill) as surface fill X,Y,Z plots to represent the point by point average, standard deviation,

minimum, maximum, and range of the population. Qualitative assessment of individual variability within corneas and across the population was performed. The Kolmogorov-Smirnov test was performed to test for non-normality of the stromal thickness data at the corneal vertex. A Student *t* test was performed to compare the stromal thickness at the corneal vertex between right eyes and left eyes. The point location of the thinnest stroma was determined for each eye (using mirrored left eyes) and the average and standard deviation of the x- and y-coordinates of the thinnest point were calculated.

The stromal thickness data for each eye were transposed to center the data on the thinnest point rather than the corneal vertex. Descriptive statistics (average and standard deviation) were recalculated and mapped for all eyes with the thinnest point as the origin. The cross-sectional hemi-meridional average stromal thickness profile was determined for each eye by averaging the stromal thickness within the 0.03-mm zone centered on the thinnest point and within 35 annular bands each 0.06-mm wide centered on the thinnest point with central radii increasing in 0.1-mm increments. The average stromal thickness within each annular band was plotted against the radial distance from the thinnest point.

To investigate the absolute stromal thickness progression from the thinnest point towards the periphery, the difference between the stromal thickness for each annular band and the thinnest stroma of each eye was calculated. The average of these differences was plotted against the radial distance from the thinnest point. Polynomial linear regression analysis was performed and the regression equation and Pearson's correlation coefficient were calculated to describe the absolute stromal thickness progression from the thinnest point to the periphery.

To investigate whether absolute stromal thickness progression was dependent on stromal thickness at the thinnest point, eyes were split into three groups: thin stroma, thick stroma, and average stromal thickness based on stromal thickness at the thinnest point. The thin stroma group consisted of patients whose stromal thickness was at least one standard deviation lower than the average stromal thickness at the thinnest point. The thick stroma group comprised patients whose stromal thickness was at least one standard deviation greater than the average stromal thickness at the thinnest point. The average stromal thickness group consisted of patients whose stromal thickness was within one standard deviation of the average stromal thickness at the thinnest point. Polynomial linear regression analysis was performed, and the regression equation and Pearson's correlation coefficient were calculated to describe the absolute stromal thickness progression from the thinnest point to the periphery for each group.

To investigate the symmetry of the absolute stromal thickness progression, directional hemi-meridional absolute stromal thickness progression was also calculated. The difference between the stromal thickness and the stroma at the thinnest point was calculated at 0.1-mm increments for eight hemi-meridians at 45° intervals: the nasal (0°) and temporal (180°) horizontal meridian, the superior (90°) and inferior (270°) vertical meridian, the superonasal (45°) and inferotemporal (225°) meridian, and the superotemporal (135°) and inferonasal (315°) meridian. The average absolute stromal thickness progression was plotted against the radial distance from the thinnest point for each of the eight hemi-meridians.

Descriptive statistics, comparative statistics, and linear regression were performed in Microsoft Excel 2003 (Microsoft Corp, Redmond, Wash). The Kolmogorov-Smirnov test for non-normality was performed using the online form at http://www.physics.csbsju.edu/stats/KS-test.n.plot_form.html. A *P* value <.05 was deemed to be statistically significant.

RESULTS

During the study period, 110 eyes of 56 patients (55 right and 55 left eyes) were included in the study. There were two patients whose other eye was excluded from the study because of a corneal scar. The population included 74% Caucasian, 17% East Indian, 5% East Asian, and 4% Black patients. The population mean age was 38.4 ± 12.0 years (median 36.1 years, range: 20.5 to 73.5 years). The mean refraction was -6.04 ± 3.58 diopters (D) sphere (range: -12.00 to $+6.00$) and -1.51 ± 1.30 D (range: 0.00 to -5.00) cylinder. Although the refraction was biased towards high myopes, the population was considered normal as all patients were free of ocular pathology other than refractive error.

The mean corneal vertex stromal thickness for all eyes was 465.4 ± 36.9 μm (95% confidence interval: 458.4 to 472.4 μm) (Table). Corneal vertex stromal thickness ranged from 385.6 to 532.1 μm for all eyes. The mean corneal vertex stromal thickness was 464.6 ± 35.9 μm for right eyes and 466.2 ± 38.2 μm for left eyes. No statistically significant difference was noted between the mean corneal vertex stromal thickness for right and left eyes ($P=0.918$). There was no statistical evidence of non-normality of the corneal vertex stromal thickness within the population using the Kolmogorov-Smirnov test for non-normality ($P=0.09$).

The maps of the average stromal thickness centered on the corneal vertex (Fig 1, first column) showed as expected that the corneal stroma was thinner in the central cornea and became increasingly thicker in the peripheral cornea. The mirrored average stromal thickness map (see Fig 1, first row, first column) demonstrated that the thinnest region was slightly displaced inferiorly and temporally with reference to the corneal vertex. The thickest regions in the superior and nasal peripheral stroma were on average 640 μm at the 4-mm radius.

Figure 2 shows the stromal thickness profile plotted for 15 eyes of the population selected at random using Microsoft Excel's random number function. The epithelial thickness profiles of the same 15 eyes have been previously published.¹⁸ Although all eyes exhibited a pattern of thinner central stroma, and increasingly thicker stroma in the periphery, there was great variation in stromal thickness between individual eyes. The minimum central stromal thicknesses varied between 391 μm (patient 8) and 520 μm (patient 10), and the maximum peripheral thickness at the 4-mm radius varied between 544 μm (patient 13) and 680 μm (patient 10).

The maps of stromal thickness standard deviation (see Fig 1, second column) showed the standard deviation of stromal thickness in the study population to vary very little within the central 6-mm diameter, only between 36 μm in the centronasal region and 42 μm in the temporal region. Maps of the minimum stromal thickness (see Fig 1, third column) demonstrated the thinnest stroma within the study population was 360 μm located 1 mm temporal to the corneal vertex. The thinnest stroma in the nasal and superior peripheral stroma within the study population was 550 μm , highlighting the stromal thickening from the center to the periphery. Maps of the maximum stromal thickness (see Fig 1, fourth column) demonstrated that the thickest stroma within the study population was in the mid-peripheral temporal region and the peripheral nasal region. The thickest stroma in these areas was 750 μm whereas the thickest central stroma within the study population was 530 μm , again highlighting the stromal thickening from the center to the periphery. Maps of the range of stromal thickness (see Fig 1, fifth column) demonstrated the largest range in stromal thickness to be in the mid-peripheral temporal region and the smallest range in the centronasal region.

Analysis of the thinnest stromal point within the central 5 mm of the cornea (Fig 3) demonstrated that for most eyes the thinnest stromal point was found in the inferotemporal cornea. The mean thinnest stromal point was displaced 0.33 mm (± 0.40) temporally and 0.17

mm (± 0.31) inferiorly with reference to corneal vertex or 0.37 mm at 207° . The average stromal thickness at the thinnest location was $461.8 \pm 37.3 \mu\text{m}$.

Figure 4 shows the average and standard deviation stromal thickness maps calculated for stromal thickness data transposed to center the data on the thinnest point rather than the corneal vertex. The central thin stromal zone appeared to be slightly asymmetrical, extending slightly further towards the periphery in the horizontal meridian than in the vertical meridian. The map of stromal thickness standard deviation showed the standard deviation of stromal thickness in the study population to vary little within the central 6-mm diameter, only between $37 \mu\text{m}$ in the inferotemporal region relative to the location of the thinnest stroma and $42 \mu\text{m}$ at the 3-mm radius from the thinnest stroma.

Figure 5 shows the cross-sectional hemi-meridional average stromal thickness profile from the thinnest point to the periphery for the study population. Figure 6 shows the average absolute stromal thickness progression relative to the thinnest stroma. Polynomial linear regression analysis showed that the absolute stromal thickness progression from the thinnest point to the periphery was described as a near perfect parabola according to the radial distance from the thinnest point, following the equation: $y = 6.411 x^2 + 2.444 x$ ($R^2 = 0.999$), where y is the absolute difference in stromal thickness relative to the thinnest point (μm) at the x (mm) radius from the thinnest point. The mean increase in stromal thickness with reference to the thinnest point was $9.4 \pm 2.7 \mu\text{m}$ at the 1-mm radius, $29.9 \pm 5.4 \mu\text{m}$ at the 2-mm radius, and $64.4 \pm 9.5 \mu\text{m}$ at the 3-mm radius. The standard deviation of the absolute stromal thickness progression was $< 7 \mu\text{m}$ within the central 5-mm diameter.

Figure 7 shows the absolute stromal thickness progression from the thinnest point to the periphery for eyes grouped into thin stroma, thick stroma, and average stromal thickness. There was no difference in the absolute stromal thickness progression between the thin stroma group, thick stroma group, and average stromal thickness group. The regression equations describing the absolute stromal thickness progression as a function of radius from the thinnest point were similar for the three groups. The absolute stromal thickness progression was independent of the stromal thickness at the thinnest point.

The directional hemi-meridional absolute stromal thickness progression analysis revealed that the rate of increase in stromal thickness from the thinnest point to the periphery was greater in the superior stroma than in the inferior stroma and greater in the nasal stroma than in the temporal stroma (Fig 8). The superior hemi-meridian was thickest, and the temporal hemi-meridian was thinnest at all radial distances from the thinnest point.

DISCUSSION

This is the first study to characterize the *in vivo* stromal thickness profile over an area of 10 mm in diameter in a population of normal eyes. Stromal thickness was measured from the anterior surface of Bowman's layer to the posterior surface of the endothelium. We found an average corneal vertex stromal thickness of $465.4 \pm 36.9 \mu\text{m}$. The thinnest stromal point was slightly displaced inferiorly and temporally with reference to the corneal vertex. The absolute stromal thickness progression from the thinnest point to the periphery showed slight variation within the study population and was independent of central stromal thickness. The absolute stromal thickness progression was slightly asymmetric with the greatest absolute stromal thickness progression in the vertical meridian and the lowest in the horizontal meridian.

Central stromal thickness has been previously measured with reported values varying between $478.3 \pm 45.6 \mu\text{m}$,² $491 \pm 35 \mu\text{m}$,³ and $498.5 \pm 29.4 \mu\text{m}$.¹ The mean value of central stromal thickness found in the present study ($465.4 \pm 36.9 \mu\text{m}$) was slightly lower than previously reported measurements obtained with a variety of optical measurement techniques. A possible

explanation for this difference is that the population of the present study was biased towards patients with thinner corneas as one of the inclusion criteria was to scan patients where the predicted residual stromal thickness was close to the 250- μm limit. However, as we demonstrated that the absolute stromal thickness progression is independent of stromal thickness at the thinnest point, the absolute stromal thickness progression reported in this study is likely to be representative of the normal population.

In the present study, we demonstrated directional differences in absolute stromal thickness progression from the thinnest point towards the periphery within the 7-mm central corneal diameter. The increase in stromal thickness was greatest in the superior meridian and lowest in the inferior meridian. Meek et al^{20,21} used x-ray scattering to map the preferred collagen orientation in the cornea and demonstrated that the central cornea was relatively uniform with respect to the amount of collagen and as a consequence in corneal thickness, whereas the peripheral corneal region might have additional collagen lamellae and might therefore be thicker.^{20,21} Meek et al suggested that the peripheral cornea might be thickest in the superior, inferior, nasal, and temporal locations.²⁰ This is not in agreement with the findings of the present study; however, it might be difficult to compare both studies as absolute stromal thickness progression was calculated with the thinnest point as the origin in the present study rather than the corneal vertex or the geometrical center of the cornea. As the thinnest point was displaced with reference to the corneal vertex, the diameter on which the absolute stromal progression could be calculated was limited to a 7-mm diameter. Thickness changes described by Meek et al appeared to occur at a larger diameter.

In the present study, we have not described the total corneal thickness profile, including the epithelium; however, it is likely that the corneal thickness profile would demonstrate similar characteristics to the stromal thickness profile in normal eyes. We previously characterized the epithelial thickness profile of the same population of eyes reported here—the epithelial thickness was found to follow a non-uniform pattern, with the 3-mm inferior epithelium 5.7 μm thicker than the 3-mm superior epithelium and 3-mm nasal epithelium 1.2 μm thicker than the 3-mm temporal epithelium.¹⁸ However, this difference represents approximately 1% of the stromal thickness and so the epithelium will make a negligible difference to corneal thickness profile relative to the stromal thickness profile in normal eyes. In contrast, the epithelium in keratoconus is known to thin over the cone^{22,23} and thicken around the cone,²³ resulting in an increased difference between the thinnest and thickest epithelium. In keratoconus, the uneven epithelial thickness profile will likely result in an increased difference between stromal thickness profile and corneal thickness profile.

Normative data of stromal thickness profiles may prove to be a useful diagnostic tool in screening for keratoconus or pellucid marginal degeneration, as these conditions are associated with localized corneal thinning.²⁴ We demonstrated that the standard deviation of the absolute stromal thickness progression from the thinnest point to the periphery was <7 μm within the central 6-mm diameter; therefore, absolute stromal thickness progression from the thinnest point towards the periphery appears to be similar in normal eyes. Any deviation from the absolute stromal thickness progression curve might indicate the presence of corneal abnormalities. In early keratoconus, assuming that peripheral stromal thickness is unchanged, the relative increase in stromal thickness between the thinnest point and the periphery might be a useful diagnostic tool. An increased difference between stromal thickness at the thinnest point and in the periphery might indicate central thinning and help diagnose early keratoconus. Previous studies have suggested using the ratio of peripheral corneal thickness to the thinnest corneal thickness as a parameter to measure the evolution of the disease.²⁵⁻²⁷ However, in these studies, peripheral thickness was measured at only one distance from the thinnest point in four meridians. The absolute stromal thickness progression provides continuous data from the thinnest point up to the 3.5-mm radius. We are currently investigating the stromal thickness

profiles of eyes with frank keratoconus and forme fruste keratoconus to attempt to subdivide forme fruste keratoconic eyes into “true” and “pseudo” keratoconic groups.

Recently, percentage increase in corneal thickness from the thinnest point towards the limbus has been suggested as a useful index for keratoconus screening.⁶ We have chosen to use the absolute stromal thickness progression rather than the percentage increase in stromal thickness. We demonstrated that absolute stromal thickness progression is independent of stromal thickness at the thinnest point. Therefore, using the percentage increase can be misleading because stromal thickness at the thinnest point varies greatly in the population. The percentage increase in stromal thickness would be greater for a thin cornea than a thick cornea, whereas we have shown that the absolute stromal thickness progression is similar for both thin and thick corneas. Using the percentage increase might then mislead the user to draw the conclusion that the thin cornea was abnormal, or that the thick cornea was normal. This is illustrated by the following example. A cornea with a thin stroma of 384 μm at the thinnest point and 466 μm at the 3.5-mm radius, and a cornea with a thick stroma of 530 μm at the thinnest point and 612 μm at the 3.5-mm radius both demonstrate the same absolute increase of 82 μm between the thinnest point and the 3.5-mm radius; however, in terms of percentage, the thin cornea shows an increase of 21.3% whereas the thick cornea shows an increase of 15.5%. This would lead to an incorrect assumption that there was a greater thickness progression in the thin cornea than the thick cornea.

Knowledge of the stromal thickness profile is of great interest in the study of corneal biomechanics in refractive surgery. The epithelium has been shown to change after refractive surgery.^{13,16,28,29} Therefore, the usefulness of studies that investigate only changes in corneal thickness are limited, as epithelial changes are not differentiated from stromal changes. The ability to characterize the stromal thickness profile will help further understand changes in stromal thickness occurring after corneal refractive surgery and may help further study biomechanical changes with the goal of increasing the accuracy of corneal refractive surgery.

This is the first published study demonstrating wide-area high-precision thickness profile analysis of the human stromal thickness in vivo. Knowledge of three-dimensional thickness mapping of the corneal stroma in a population of normal eyes provides normative data of absolute stromal thickness progression and could be of significant help in screening for corneal abnormalities such as keratoconus. Knowledge of the stromal thickness profile could also be used for biomechanical studies and gradient optical modeling of the cornea.

Acknowledgments

Supported in part by NIH grant EB000238 and the Dyson Foundation, Millbrook, NY.

References

1. Patel S, McLaren J, Hodge D, Bourne W. Normal human keratocyte density and corneal thickness measurement by using confocal microscopy in vivo. *Invest Ophthalmol Vis Sci* 2001;42:333–339. [PubMed: 11157863]
2. Patel SV, McLaren JW, Hodge DO, Bourne WM. Confocal microscopy in vivo in corneas of long-term contact lens wearers. *Invest Ophthalmol Vis Sci* 2002;43:995–1003. [PubMed: 11923239]
3. Erie JC, Patel SV, McLaren JW, Ramirez M, Hodge DO, Maguire LJ, Bourne WM. Effect of myopic laser in situ keratomileusis on epithelial and stromal thickness: a confocal microscopy study. *Ophthalmology* 2002;109:1447–1452. [PubMed: 12153794]
4. Reinstein DZ, Archer T. Combined Artemis very high-frequency digital ultrasound-assisted transepithelial phototherapeutic keratectomy and wavefront-guided treatment following multiple corneal refractive procedures. *J Cataract Refract Surg* 2006;32:1870–1876. [PubMed: 17081871]

5. Reinstein DZ, Srivannaboon S, Archer TJ, Silverman RH, Sutton H, Coleman DJ. Probability model of the inaccuracy of residual stromal thickness prediction to reduce the risk of ectasia after LASIK part I: quantifying individual risk. *J Refract Surg* 2006;22:851–860. [PubMed: 17124879]
6. Ambrosio R Jr, Alonso RS, Luz A, Coca Velarde LG. Corneal-thickness spatial profile and corneal-volume distribution: tomographic indices to detect keratoconus. *J Cataract Refract Surg* 2006;32:1851–1859. [PubMed: 17081868]
7. Mandell RB, Polse KA. Keratoconus: spatial variation of corneal thickness as a diagnostic test. *Arch Ophthalmol* 1969;82:182–188. [PubMed: 5796090]
8. Maldonado MJ, Ruiz-Oblitas L, Munuera JM, Aliseda D, Garcia-Layana A, Moreno-Montanes J. Optical coherence tomography evaluation of the corneal cap and stromal bed features after laser in situ keratomileusis for high myopia and astigmatism. *Ophthalmology* 2000;107:81–88. [PubMed: 10647724]
9. Wirbelauer C, Pham DT. Monitoring corneal structures with slitlamp-adapted optical coherence tomography in laser in situ keratomileusis. *J Cataract Refract Surg* 2004;30:1851–1860. [PubMed: 15342046]
10. Moller-Pedersen T, Vogel M, Li HF, Petroll WM, Cavanagh HD, Jester JV. Quantification of stromal thinning, epithelial thickness, and corneal haze after photorefractive keratectomy using in vivo confocal microscopy. *Ophthalmology* 1997;104:360–368. [PubMed: 9082257]
11. Li HF, Petroll WM, Moller-Pedersen T, Maurer JK, Cavanagh HD, Jester JV. Epithelial and corneal thickness measurements by in vivo confocal microscopy through focusing (CMTF). *Curr Eye Res* 1997;16:214–221. [PubMed: 9088737]
12. Gokmen F, Jester JV, Petroll WM, McCulley JP, Cavanagh HD. In vivo confocal microscopy through-focusing to measure corneal flap thickness after laser in situ keratomileusis. *J Cataract Refract Surg* 2002;28:962–970. [PubMed: 12036637]
13. Reinstein DZ, Silverman RH, Raevsky T, Simoni GJ, Lloyd HO, Najafi DJ, Rondeau MJ, Coleman DJ. Arc-scanning very high-frequency digital ultrasound for 3D pachymetric mapping of the corneal epithelium and stroma in laser in situ keratomileusis. *J Refract Surg* 2000;16:414–430. [PubMed: 10939721]
14. Cusumano A, Coleman DJ, Silverman RH, Reinstein DZ, Rondeau MJ, Ursea R, Daly SM, Lloyd HO. Three-dimensional ultrasound imaging. Clinical applications. *Ophthalmology* 1998;105:300–306. [PubMed: 9479291]
15. Reinstein DZ, Couch DG, Archer T. Direct residual stromal thickness measurement for assessing suitability for LASIK enhancement by Artemis 3D very high-frequency digital ultrasound arc scanning. *J Cataract Refract Surg* 2006;32:1884–1888. [PubMed: 17081873]
16. Reinstein DZ, Ameline B, Puech M, Montefiore G, Laroche L. VHF digital ultrasound three-dimensional scanning in the diagnosis of myopic regression after corneal refractive surgery. *J Refract Surg* 2005;21:480–484. [PubMed: 16209446]
17. Reinstein DZ, Srivannaboon S, Holland SP. Epithelial and stromal changes induced by Intacs examined by three-dimensional very high-frequency digital ultrasound. *J Refract Surg* 2001;17:310–318. [PubMed: 11383762]
18. Reinstein DZ, Archer TJ, Gobbe M, Silverman RH, Coleman DJ. Epithelial thickness in the normal cornea: three-dimensional display with Artemis very high-frequency digital ultrasound. *J Refract Surg* 2008;24:571–581. [PubMed: 18581782]
19. Reinstein DZ, Silverman RH, Coleman DJ. High-frequency ultrasound measurement of the thickness of the corneal epithelium. *Refract Corneal Surg* 1993;9:385–387. [PubMed: 8241045]
20. Aghamohammadzadeh H, Newton RH, Meek KM. X-ray scattering used to map the preferred collagen orientation in the human cornea and limbus. *Structure* 2004;12:249–256. [PubMed: 14962385]
21. Meek KM, Tuft SJ, Huang Y, Gill PS, Hayes S, Newton RH, Bron AJ. Changes in collagen orientation and distribution in keratoconus corneas. *Invest Ophthalmol Vis Sci* 2005;46:1948–1956. [PubMed: 15914608]
22. Scroggs MW, Proia AD. Histopathological variation in keratoconus. *Cornea* 1992;11:553–559. [PubMed: 1468218]

23. Reinstein, DZ.; Archer, TJ.; Gobbe, M. Exclusion of keratoconus initially diagnosed by Orbscan using epithelial and stromal layer thickness mapping. Presented at: American Academy of Ophthalmology Annual Meeting; November 11-14, 2006; Las Vegas, Nev.
24. Nottingham, J. Practical Observations on Conical Cornea and on the Short Sight, and Other Defects of Vision Connected with It. London: John Churchill; 1854.
25. Avitabile T, Marano F, Uva MG, Reibaldi A. Evaluation of central and peripheral corneal thickness with ultrasound biomicroscopy in normal and keratoconic eyes. *Cornea* 1997;16:639–644. [PubMed: 9395873]
26. Avitabile T, Franco L, Ortisi E, Castiglione F, Pulvirenti M, Torrisi B, Castiglione F, Reibaldi A. Keratoconus staging: a computer-assisted ultrabiomicroscopic method compared with videokeratographic analysis. *Cornea* 2004;23:655–660. [PubMed: 15448489]
27. Gromacki SJ, Barr JT. Central and peripheral corneal thickness in keratoconus and normal patient groups. *Optom Vis Sci* 1994;71:437–441. [PubMed: 7970558]
28. Reinstein DZ, Silverman RH, Sutton HF, Coleman DJ. Very high-frequency ultrasound corneal analysis identifies anatomic correlates of optical complications of lamellar refractive surgery: anatomic diagnosis in lamellar surgery. *Ophthalmology* 1999;106:474–482. [PubMed: 10080202]
29. Reinstein D, Srivannaboon S, Gobbe M, Archer T, Silverman R, Sutton H, Coleman DJ. Epithelial thickness profile changes induced by myopic LASIK as measured by Artemis very high-frequency digital ultrasound. *J Refract Surg*. In press

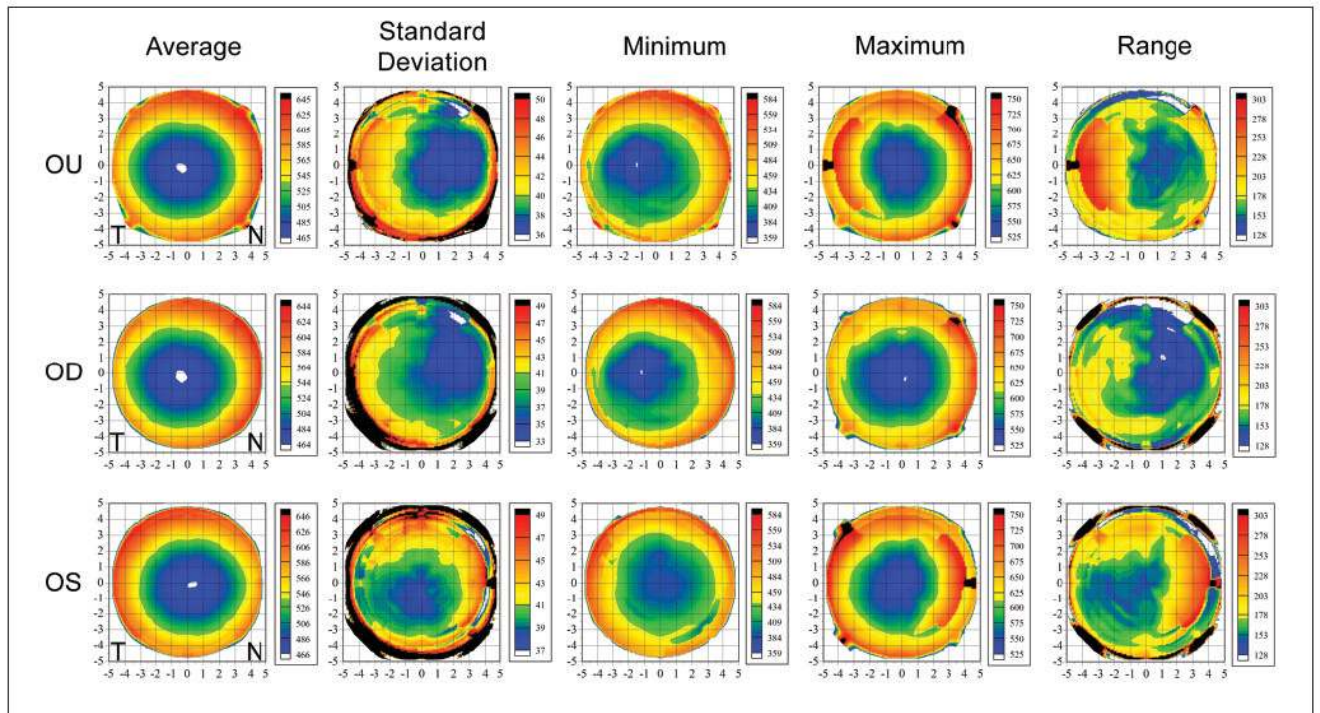


Figure 1. Topographical map of the descriptive statistics of stromal thickness centered on the corneal vertex for the population. The color scale represents the stromal thickness in microns. A Cartesian 1-mm grid is superimposed with the origin at the corneal vertex.

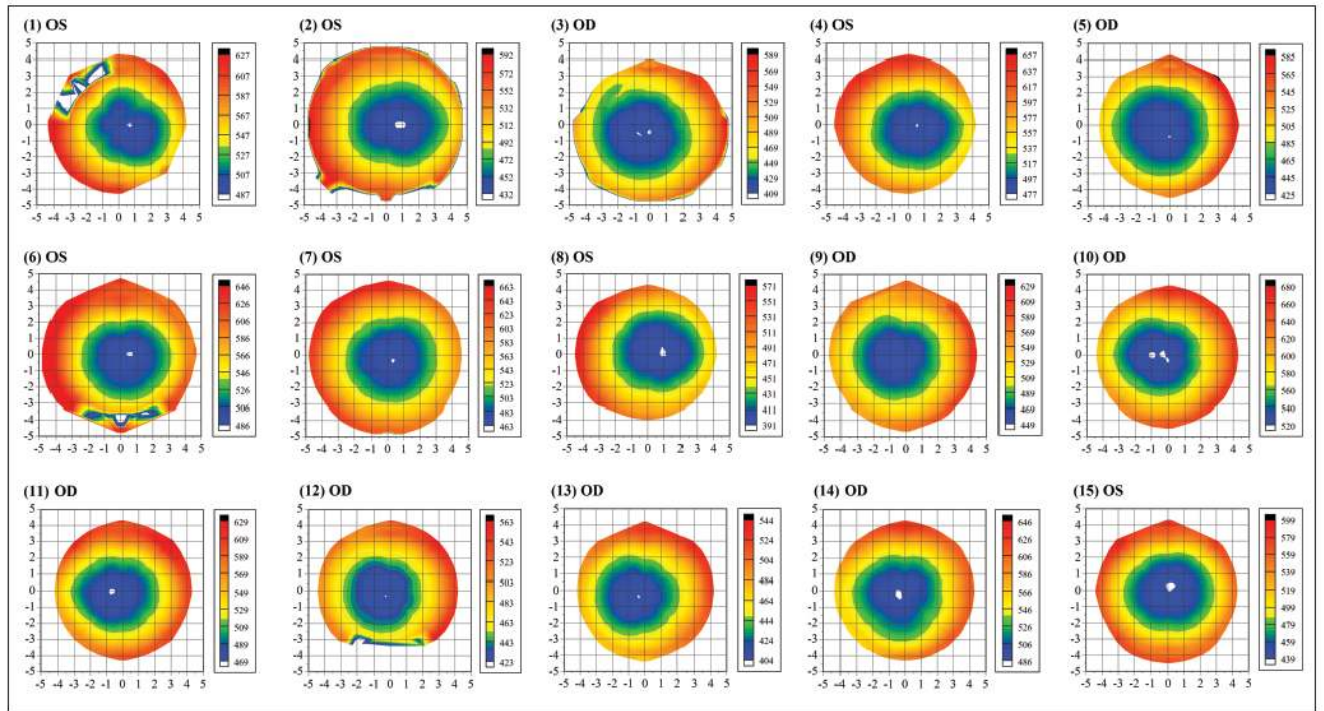


Figure 2. Stromal thickness maps of 15 randomly selected eyes each plotted with an individual color scale representing the stromal thickness in microns. A Cartesian 1-mm grid is superimposed with the origin at the corneal vertex. The epithelial thickness profiles of the same 15 eyes have been published previously.¹⁸

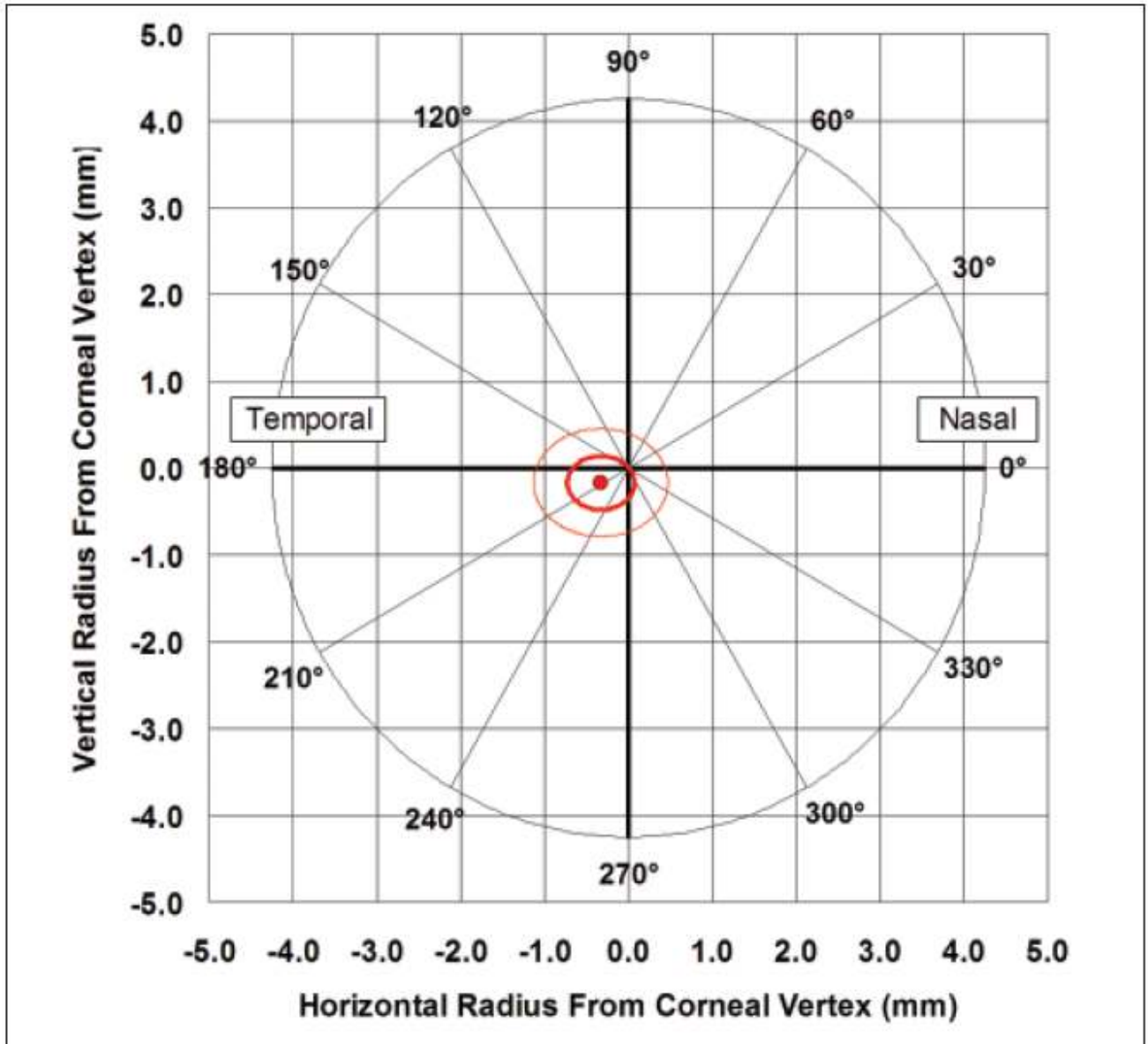


Figure 3.

Average location of the thinnest stroma within the central 5 mm of the cornea. The red dot represents the average location of the thinnest stroma for all eyes tested. The thick red ellipse represents one standard deviation in the x- and y-directions and the thin red ellipse represents two standard deviations in the x- and y-directions. A Cartesian 1-mm grid is superimposed with the origin at the corneal vertex. Positive x values represent the nasal stroma and negative values represent the temporal stroma. Positive y values represent the superior stroma and negative values represent the inferior stroma.

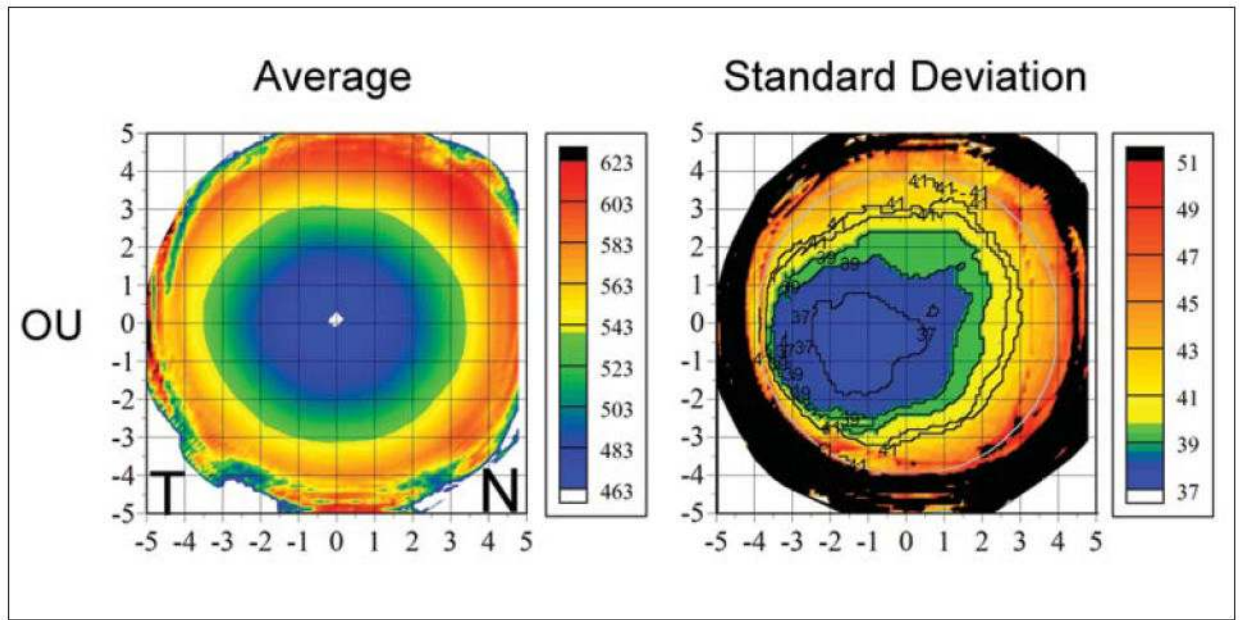


Figure 4.

Topographic map of the average and standard deviation of stromal thickness for the population centered on the thinnest point. The color scale represents the stromal thickness in microns. A Cartesian 1-mm grid is superimposed with the origin at the thinnest point. Both maps include all eyes with left eyes mirrored (positive x-values represent the nasal stroma and negative values represent the temporal stroma).

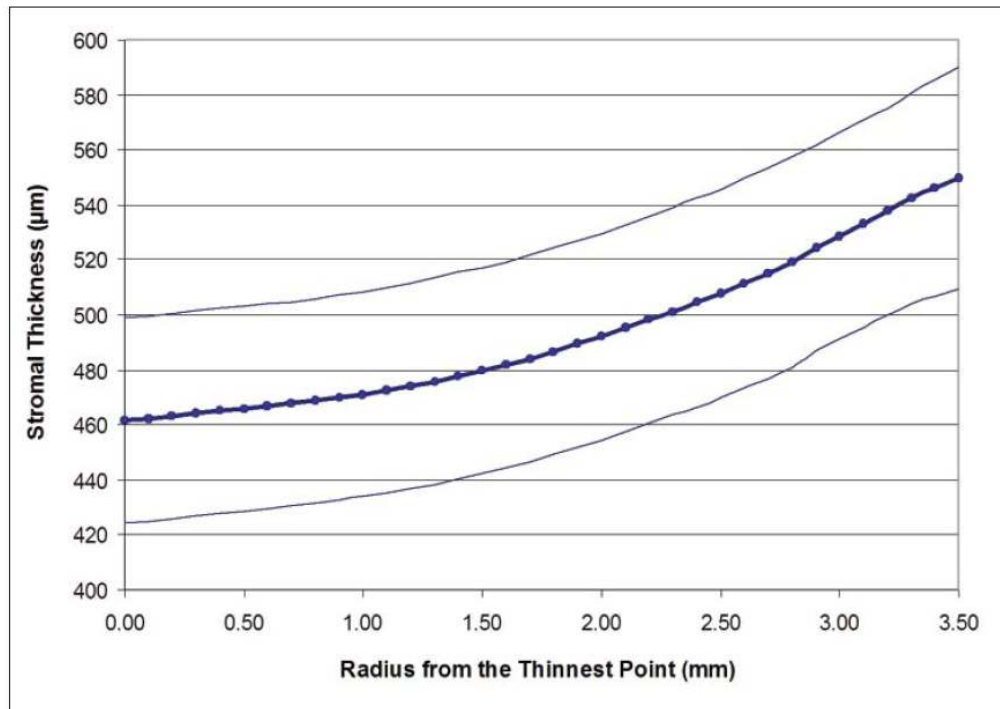


Figure 5. Cross-sectional hemi-meridional average stromal thickness profile (μm) for 110 eyes using mirrored left eye symmetry. The data points represent the average stromal thickness of all data within an annulus of a given radius. The x axis is the radial distance (mm) from the location of the thinnest point. The thick blue line represents the average stromal thickness profile. The thin blue lines represent one standard deviation less than and one standard deviation greater than the average stromal thickness.

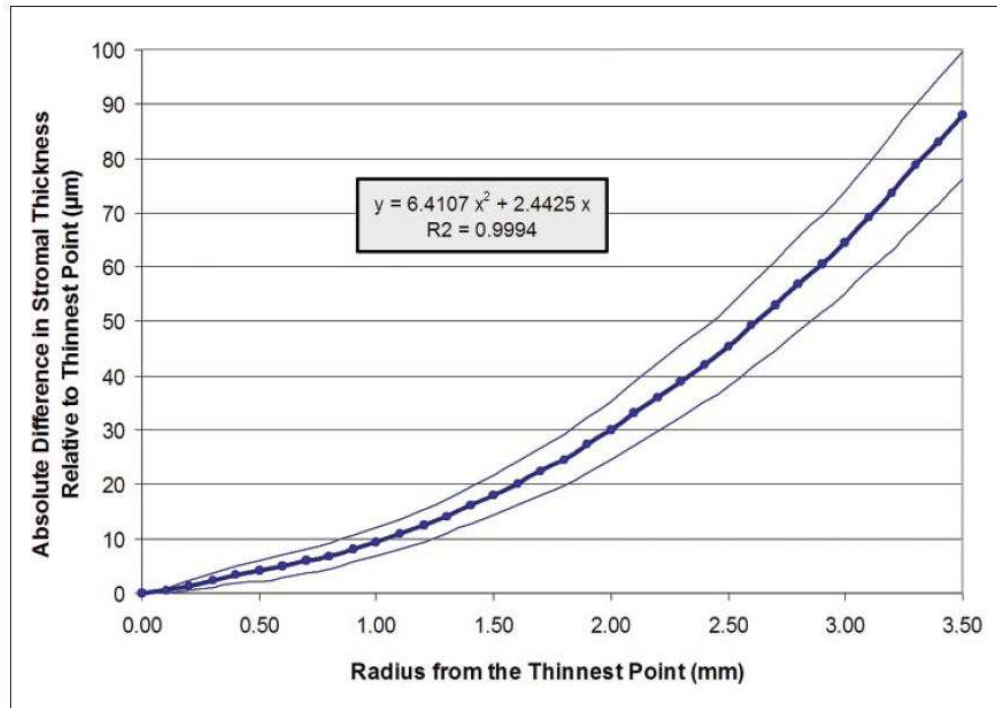


Figure 6.

Average absolute stromal thickness progression (μm) with reference to the thinnest point for 110 eyes using mirrored left eye symmetry. The data points represent the difference between the average stromal thickness of all data within an annulus of a given radius and the thinnest stromal thickness. The x axis is the radial distance (mm) from the location of the thinnest point. The thick blue line represents the absolute stromal thickness progression. The thin blue lines represent one standard deviation less than and one standard deviation greater than the absolute stromal thickness progression.

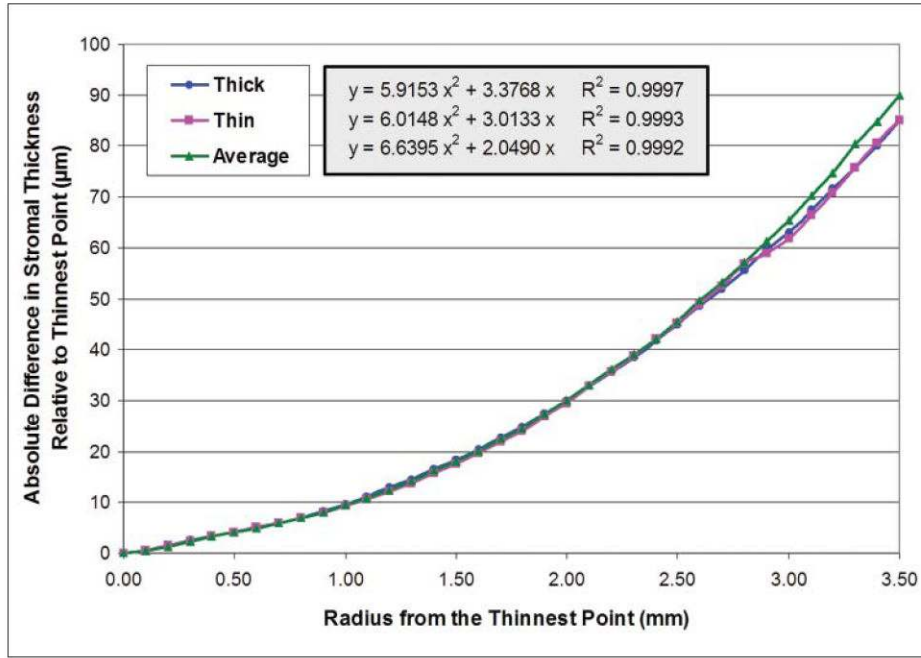


Figure 7. Average absolute stromal thickness progression (μm) with reference to the thinnest point for 110 eyes using mirrored left eye symmetry grouped as thin, average, and thick central stromal thickness. The data points represent the difference between the average stromal thickness of all data within an annulus with a given radius and the value at the thinnest point. The x axis is the radial distance (mm) from the thinnest point location. The thin stroma group consisted of patients whose stromal thickness was at least one standard deviation less than the average stromal thickness at the thinnest point and is represented by the pink line. The thick stroma group consisted of patients whose stromal thickness was at least one standard deviation greater than the average stromal thickness at the thinnest point and is represented by the blue line. The average stroma group consisted of patients whose stromal thickness was within one standard deviation of the mean and is represented by the green line.

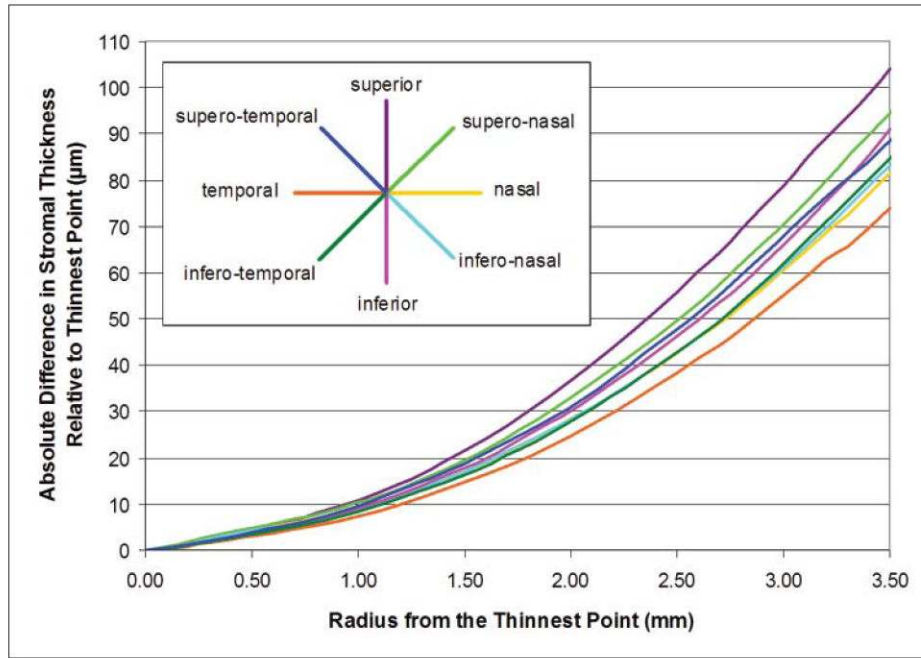


Figure 8. Average absolute stromal thickness progression (μm) with reference to the thinnest point in eight hemi-meridians for 110 eyes using mirrored left eye symmetry. The data points represent the difference between the average stromal thickness of all data within an annulus with a given radius and the value at the thinnest point. The x axis is the radial distance (mm) from the thinnest point location. Each line represents the absolute stromal thickness progression along a given hemi-meridian, in eight hemi-meridians at 45° intervals.

TABLE

Corneal Vertex Stromal Thickness

	Corneal Vertex Stromal Thickness (μm)		
	All Eyes	Right Eyes	Left Eyes
Mean \pm SD	465.4 \pm 36.9	464 \pm 35.9	466.2 \pm 38.2
Minimum	385.6	385.8	38.6
Maximum	532.1	527.	532.1
Range	146.5	141.4	146.5